RSC Advances

ROYAL SOCIETY OF CHEMISTRY

www.rsc.org/advances

One step synthesis cadmium sulphide/reduced graphene oxide sandwiched film modified electrode for simultaneous electrochemical determination of hydroquinone, catechol and resorcinol

Shirong Hu[a,b], Wuxiang Zhang[b], Jianzhong Zheng[b], Jiangu Shi[b], Zhongqiu Lin[b], Ling Zhong[b], Guixiang Cai[b], Chan Wei[b], Hanqiang Zhang[b], Aiyou Hao[a*]

[a] School of Chemistry and Chemical Engineering, Shandong University, Jinan 250100, P.R. China.

[b] College of Chemistry and Environment, Minnan Normal University, Zhangzhou 363000, P.R. China.

* Corresponding author: Tel: +86 531 88363306. Fax: +86 531 8564464

E-mail address: haoay@sdu.edu.cn (prof. A. Hao).

Abstract In this work, a novel sandwiched film of cadmium sulphide/reduced graphene oxide (CdS/r-GO) was synthesized via one step hydro-thermal reaction and the modified electrode of composite was successfully used to simultaneously determine hydroquinone (HQ), catechol (CC) and resorcinol (RC). Additionally, some kinetic parameters, such as charge transfer coefficient (α) and the electron transfer rate constant (k_s) were calculated. Differential pulse voltammetry (DPV) was used for the simultaneous determination of HQ, CC and RC in their ternary mixture. The calibration curves of HQ, CC and RC were obtained in the range of 0.2 to 2300 μM, 0.5 to 1350 μM and 1.0 to 500 μM, respectively. And the detection limits for HQ, CC and RC were 0.054 μM, 0.09 μM and 0.23 μM (S/N=3). Then the modified electrode was applied to detect the tap water, well water and river water and the results show that the significance of practical application in the aquatic environment.

Keywords cadmium sulphide; reduced graphene oxide; electrochemistry; dihydroxybenzene isomers; simultaneous determination

1. Introduction

Hydroquinone (HQ), catechol (CC) and resorcinol (RC) are three isomers of dihydroxybenzene, which are widely used in metallurgy, pharmacy, petroleum chemical industry, plastic and other related industries.[1-3] Moreover, they are low degradability and can have deleterious effects on the vegetation, animal and human life, which inadvertently released into the environment when manufacturing process of industrial compounds. Researches show that human health, animals, plants and aquatic life may be threatened if ingestion a certain amount of dihydroxybenzene isomers.[4-6] So they are considered as environmental pollutants by the US Environmental Protection Agency (EPA) and the European Union (EU).[7] Thus, development the fast and convenient analytical methods for determination of dihydroxybenzene isomers are imperative. However, similar structures and properties of HQ, CC and RC make it hard for identification each other, so determination of dihydroxybenzene isomers is of great practical significance.[8]

So far, various techniques have been employed for the simultaneous determination of dihydroxybenzene isomers including chromatography,[9,10] spectrophotometry,[11] synchronous fluorescence[12,13] and electrochemical methods,[14] and so on. Among these methods, the electrochemical technique is the most efficient method in the simultaneous determination of dihydroxybenzenes isomers due to its excellent properties such as simple operation, high sensitivity and low cost. As far as we know, simultaneous determination of HQ, CC and RC with the width of linearity direction are still a big problem because of among of them have very similar structures and the overlap oxidation potentials.[15,16] Thus, we design appropriate materials to improve the selectivity of working electrode and widen the linear range.

Carbon nanocomposites such as carbon nanotube[17], carbon nanofiber[18] and functionalized graphene are considered as ideal matrices in the fabrication of electrochemical sensors. Among of them, graphene, as a class of 'two-dimensional' (2D) carbon nanomaterial, have recently received considerable attention because of their advantageous characteristics of uniform and tailored pore structure, high theoretical surface and excellent electronic conductivity.[19-21] Moreover, integrated graphene into self-assembly graphene-based composites not only can promote the electron transfer rate, but also strengthen to their synergistic interaction in

graphene-based composites. For example, Huang and coworkers synthesized (AgNPs)–polydopamine@graphene composites and used as high-performance electrochemical detection,[22] Yu and coworkers synthesized Graphene/MoS_2 nanoflake were used as Lithium-ion battery,[23] Li et al. introduced CdS-cluster-graphene into photocatalytic hydrogen production,[24] ect. These reports demonstrate well that the combination between graphene and other different materials have the possibility to form different types of graphene-based hybrid materials. As a class of transition-metal dichalcogenides, cadmium sulfide (CdS) have recently received considerable attention because of their advantageous bandgap and quantum size characteristics. The electron-hole species can efficiently transport electron on the surface of CdS.[25,26] Specifically, high-quality CdS nanoparticles are of great interest to employed to develop biosensor.[27,28]

In this paper, we applied one-step reaction to fabricate sandwiched structured cadmium sulphide/reduced graphene oxide (CdS/r-GO) films modified electrode were used as simultaneous detection of dihydroxybenzene isomers for the first time. The calibration curves for HQ, CC and RC were obtained in the wide range of 0.2 to 2300 μM, 0.5 to 1350 μM and 1.0 to 500 μM, respectively. With the low limits of detection for HQ, CC and RC were 0.054 μM, 0.09 μM and 0.23 μM (S/N=3). Then the CdS/r-GO was further applied in the determination of dihydroxybenzene isomers in the practical aquatic environment.

2. Experimental

2.1. Reagents and apparatus

Graphite powder, sodium nitrate, potassium permanganate, hydrochloric acid, sulfuric acid, hydrogen peroxide (30%) and phosphate buffer solution were purchased from Sinopharm Chemical Reagent Co., Ltd. Hydroquinone (HQ), catechol (CC) and resorcinol (RC), cadmium carbonate and acetic acid were purchased from Xilong Chemical Co., Ltd. All other reagents are analytical reagents. All aqueous solutions were prepared using ultrapure water (18 MΩ·cm) from a Milli-Q system (Millipore).

Scanning electron microscopy (SEM) and energy dispersive X-ray spectroscopy (EDS) were conducted on JEM-6010La. Atomic force microscope (AFM) images were obtained with CSPM 5500 scanning probe microscope (China). All electrochemical measurements were performed on

a CHI660E electrochemical workstation (Chenhua Co., Shanghai, China). The glassy carbon electrode (CHI104, d = 3mm) was used as working electrode. The Ag/AgCl electrode and platinum wire were used as reference and auxiliary electrodes, respectively.

2.2. Synthesis of cadmium sulphide/reduced graphene oxide composite materials

The graphene oxide (GO) was synthesized from natural graphite by a modified Hummers' method, which has been reported previously.[29] The GO was dispersed in water (10 g L^{-1}), then cadmium acetate synthesized by 0.2 mM L^{-1} $CdCO_3$ and a certain amount of ethylic acid solution. Then GO (4 mL) cadmium acetate were dispersed in 30 mL dimethylsulfoxide (DMSO) under vigorous ultrasonic (40 kHz, 500 W) for 20 min until the homogeneous mixing of solution. Then transferred into a 45 ml autoclave and heated at 180 °C for 6 h. Catalyzing reduce GO into r-GO by high temperature and high pressure during the reaction. The brownish-green cadmium sulphide/reduced graphene oxide (CdS/r-GO) products were obtained and washed several times with water and ethanol and then oven dried at 80 °C.

2.3. Modification of electrodes

Firstly, the glassy carbon electrode was polished to a mirror-like finish with 1.0, 0.3 and 0.05 μm alumina powder, respectively and thoroughly cleaned before use. Then, 6.0 μL of CdS/r-GO solution was droped on the surface of working electrode, and dried the surface of CdS/r-GO of glassy carbon electrode with room temperature.

3. Results and discussion

3.1. Characterization of GO and CdS/r-GO composite material

The surface morphologies of graphene oxide (GO) and the CdS/r-GO film were investigated by scanning electron microscope (SEM). As shown in **Fig. 1A**, the product of GO were sheet morphology, which was in agreement with that reported previously.[30,31] Then CdS/r-GO consisted of layer-layer graphene sheets decorated with CdS. Wrinkles of CdS/r-GO, a characteristic feature of the graphene sheets, were observed in **Fig. 1B**. Besides, the result of EDS indicated that the CdS/r-GO contain mainly carbon, oxygen, sulphur and cadmium without any observable impurities were detected in **Fig. 1C**, which indicated that CdS decorated r-GO

film had been successfully synthesized by a one-step process.

Fig. 1

Atomic force microscope (AFM) images of the r-GO/GCE and the CdS/r-GO/GCE film were shown in **Fig. 2.** It is observed that the r-GO/GCE was layer structure and relatively smooth with an average roughness of 35.7 nm (**Fig. 2A**). However, on CdS/r-GO/GCE (**Fig. 2B**), the surface was irregular spinous islands and lots of adjacent peaks with the average roughness of 146 nm, which was obviously larger than that (35.7 nm) on bare r-GO/GCE, indicated the morphology of modified electrode had changed. The profile line showed the highest and lowest peaks of r-GO/GCE were 615.5 nm and 470.8 nm. And CdS/r-GO/GCE were 1191.2 nm and 475.5 nm, respectively. The differences of roughness and section features demonstrated that the r-GO and CdS/r-GO had been successfully modified on the electrode and improved the surface effect of the electrode interface.

Fig. 2

3.2. Characterization of electrochemical behavior of CdS/r-GO/GCE.

The electrochemical properties for different electrodes of GCE, r-GO/GCE and CdS/r-GO/GC were determined from cyclic voltammograms (CV). As illustrated in **Fig. 3,** the oxidation peak current of dihydroxybenzene isomers increased significantly on CdS/r-GO/GCE. A possible reaction mechanism was discussed here as shown in **Scheme 1**. It is generally known that transition-metal CdS not only have excellent electrical conductivity of the semiconductor materials, but also act as an electron transfer channel, accelerating the electron transfer between the surface of r-GO and the CdS. The sp^2 and sp^3 hybridized carbon-carbon bonds of r-GO provided high level of conductivity and redox in the electrochemical reaction.[32-35] By chemical valence combining sandwich structure would be expected to hold good electron conductivity, low diffusion resistance to protons/cations, easy electrolyte penetration, and high electroactive areas to provide a homogenous environment for the fabrication of high performance

electrochemical sensor.[36-38] So the CdS/r-GO modified electrode had more stable electrical signal, specificity and higher repeatability dihydroxybenzenes isomers.

Fig. 3

Scheme 1

3.3. Effect of pH

The effect of pH value on the electrochemical behavior of 0.2 mM HQ, 0.2 mM CC and 0.2 mM RC in the mixed solution at CdS/r-GO/GCE was investigated by CV in pH increased ranging from 4.0 to 8.5. As shown in **Fig. 4,** it could be seen that the oxidation peak current of HQ, CC and RC increased with increasing pH value until it reached 7.0, and then the oxidation peak currents decreased when the pH increases further. In weak acid, the CdS/r-GO would be protonated and the hydroxyl in dihydroxybenzene did not ionized, which decreased the adsorption capacity of dihydroxybenzene isomers and producted highly overpotential. In alkaline solution, the dihydroxybenzene isomers were instable, which easily been oxidized and effected the detection of target molecules. Therefore, 7.0 of pH was chosen as the subsequent optimal analytical experiments.

The relationship between the peak potential E_{pa} and pH on the CdS/r-GO/GCE was also investigated and the results were shown in **Fig.4**. For HQ, the linear equation was E_{pa}/V = -0.0574 pH + 0.518 (R = 0.9968); the CC linear equation was E_{pa}/V = -0.0623 pH + 0.6412 (R = 0.9982); For RC, The follow the equation of E_{pa}/V = -0.0652 pH + 1.057 (R = 0.9987). The slopes of the three regression equations were approximate with the theoretical value -0.059 V/pH of Nernstian. It indicated that the electrochemical oxidize of HQ, CC and RC on CdS/r-GO/GCE should be a two electrons and two protons process.[39]

Fig. 4

3.4. Effects of scan rate

In the following experiment, scan rate of HQ, CC and RC (CV of 0.2 mM on the CdS/r-GO/GCE with different scan rate) was investigated to better understand the

electrochemical mechanism on CdS/r-GO/GCE. As shown in **Fig. 5**, the redox peak current of dihydroxybenzene isomers increased linearly of scan rate in the range of 0.01-0.4 V s^{-1}. Moreover, with the increase of scan rate, the redox potential of HQ, CC and RC shifted positively. For HQ, the linear relationship between redox potential and the scan rate were I_{pa} (μA) = -112.88 υ (V s^{-1}) - 2.341 (R = 0.9972) and I_{pc} (μA) = 121.73 υ (V s^{-1}) + 5.592 (R = 0.9972). For CC, the linear equations were I_{pa} (μA) = -125.47 υ (V s^{-1}) - 6.926 (R = 0.9965) and I_{pc} (μA) = 83.12 υ (V s^{-1}) + 2.149 (R = 0.9976). Bur for RC, only an oxidation peak, which showed the oxidation process were irreversible electrode process, the linear regression equations of RC could be expressed as I_{pa} (μA) = -136.9 υ (V s^{-1}) - 9.784 (R = 0.9973), which indicated that the redox of HQ, CC and RC on CdS/r-GO/GC were typical adsorption-controlled processes.[40]

For the reversible electrochemical process, The dependence of the potential and scan rate could be described according to Laviron theory: [41]

$$\log \frac{k_a}{k_c} = \log \frac{\alpha}{1-\alpha} \text{ or } \frac{k_a}{k_c} = \frac{\alpha}{1-\alpha} \quad (1)$$

where k_a and k_c was the slope of the straight lines for E_{pa} versus logυ and E_{pc} versus logυ, respectively. In this work, the E_{pa} and E_{pc} were linearly dependent on the logυ with the regression equations of E_{pa} (V) = 0.027 logυ (V s^{-1}) +0.133 (R = 0.9989) and E_{pc} (V) = -0.021 logυ (V s^{-1}) - 0.015 (R = 0.995) for HQ and E_{pa} (V) = 0.026 logυ (V s^{-1}) +0.239 (R = 0.9945) and E_{pc} (V) = -0.012 logυ (V s^{-1}) - 0.0153 (R = 0.9947) for CC. Thus, α was calculated to be 0.563 and 0.684 for HQ and CC, The apparent heterogeneous electron transfer rate constant (k_s) could also be obtained according to the E_q:[42,43]

$$\log k_s = \alpha \log(1-\alpha) + (1-\alpha)\log\alpha - \log\frac{RT}{nFv} - \frac{\alpha(1-\alpha)nF\Delta E_p}{2.3RT} \quad (2)$$

where n was the number of electrons involved in the reaction, and $\triangle E_p$ was the peak-to-peak potential separation was 0.11, other symbols had their usual meanings. The number of electrons involved in the reaction of HQ and CC were 2. Thus, the values of k_s were calculated to be 0.462 cm s^{-1} and 0.539 cm s^{-1} for HQ and CC, respectively. These results indicated that the CdS/r-GO composite material can effectively promote the electron transfer.

For RC, the relationship between the anodic peak potential (E_{pa}) and the natural logarithm of the scan rate (lnυ) was constructed and followed the linear regression equation of E_{pa} (V) = 0.012

lnυ (mV s^{-1}) + 0.65 (R = 0.9969). For a irreversible electrode process, the relationship between E_{pa} and lnυ was expressed as follows by Laviron:

$$E_{\mathrm{pa}} = E_o + \left(\frac{RT}{\alpha nF}\right) \ln\left(\frac{RTk^o}{\alpha nF}\right) + \left(\frac{RT}{\alpha nF}\right) \ln v \quad (3)$$

where E_o was standard electrode potential, α was charge transfer coefficient, n was transfer electron number, R, T and F had their usual meanings. Because the electron number involved in the oxidation process is 2, α was calculated to be 0.35.

Fig. 5

3.5. Differential pulse voltammetry simultaneous determination of HQ, CC and RC

Differential pulse voltammetry (DPV) was quantitative determination of HQ, CC and RC. As shown in **Fig.6**, under the optimal conditions, the individual determination of HQ, CC, or RC in their mixtures were investigated when the concentration of one species changed, whereas those of other two species remained constant. **Fig. 6A** showed the DPV of HQ with different concentrations in the presence of 0.2 mM CC and 0.2 mM RC. Two linear regression equations were also obtained which were calculated as I_{pa} (μA) = -0.0897 C(μM) - 21.08 (0.2 to 60 μM, R = 0.9956). And I_{pa} (μA) = -0.0123 C(μM) - 27.186 (60 to 2300 μM, R = 0.9979). Similarly, as shown in **Fig. 6B**, keeping the concentration of HQ and RC constant (0.2 mM), the oxidation peak current increased linearly with increasing the concentration of CC in the range of I_{pa} (μA) = -0.0327 C(μM) - 18.57 (0.5 to 1350 μM, R = 0.9965). The **Fig. 6C** showed the DPV of RC with different concentrations in the presence of 0.2 mM HQ and 0.2 mM CC, the linear egression equation was calibrated as I_{pa} (μA) = -0.0398 C(μM) - 8.489 (1.0 to 500 μM, R = 0.9947). The detection limits of blank (S/N=3) for the determination of HQ, CC and RC were evaluated as 0.054 μM, 0.09 μM and 0.23 μM. Thus, the selective and sensitive determination of HQ, CC and RC were achieved simultaneously at CdS/r-GO/GCE.

Fig. 6

3.6. Interference and repeatability studies

Some common interference for the simultaneous determination of HQ CC and RC were investigated, such as NaCl, K_2SO_4, $MgCl_2$ solutions (150 fold), phenol, nitrophenol and glucose solutions (100 fold). The oxidation peak potential and current of HQ, CC and RC were observed almost constantly. In addition, the modified electrode determined dihydroxybenzene isomers sample in every four days. The **Fig. 7** showed that electrochemical sensor could keep its activity for almost a month. Moreover, The comparison of the proposed method with other electrochemical methods reported for the determination was summarized in **Table 1**. And compared to HPLC methods, this sensors has a wider detection range and lower detection limits.[44] Thus, our simple and inexpensive method was very promising in the determination of dihydroxybenzene isomers. Thus, the results indicated the CdS/r-GO/GCE exhibited good selectivity for detection of dihydroxybenzene isomers.

Fig. 7

Table 1

3.7. Application of the method to analysis samples

For the further evaluation of the applicability of the method tap water, well water and local river water samples were used for quantitative analysis after filtering with a cellulose membrane filter (pore size 0.25 μm) for several times. then 5 mL of the real samples were diluted to 10 mL with 0.1 mM PBS solutions. The results were shown in **Table 2.** The recovery of the spiked samples ranged between 96.8% and 102.7% (n=6). The results indicated practical applicability of CdS/r-GO/GCE for simultaneous determination of HQ, CC and RC in practice water samples.

Table 2

4. Conclusions

In summary, the CdS/r-GO sandwiched film composites were firstly designed as support matrix for the construction of electrochemical sensor for simultaneous determination of HQ,

CC and RC. Three pairs of independently redox peaks was obtained. The value of charge transfer coefficient (α) and the electron transfer rate constant (k_s) were calculated. And the CdS/r-GO/GCE exhibited a low detection limit and wide linear range, and the detection limits for HQ, CC, and RC were 0.054 μM, 0.09 μM and 0.23 μM (S/N=3), respectively. The recovery of the water samples ranged between 96.8% and 102.7%, which could provide a promising platform for the quantitative determination of HQ, CC and RC in micromole level of practical water samples.

Acknowledgments

This project was supported by Fujian Province Natural Science Foundation (2012D136), National Undergraduate Innovative Training Program (201410402002), The Science and Technology Foundation of Fujian Provincial Bureau Quality and Technical Supervision (NO.FJQI 2013108).

References

1 D. Zhao, X. Zhang, L. Feng, L. Jia and S. Wang, Colloid. Surface B, 2009, 74, 317–321.

2 Y. Du, M. Zhou and L. Lei, J. Hazard. Mater., 2006, 136, 859–865.

3 H. L. Guo, S. Peng, J. H. Xu, Y. Q. Zhao and X. Kang, Sens. Actuators, B, 2014, 193, 623–629.

4 Y. Quan, Z. Xue, H. Shi, X. Zhou, J. Du and X. Lu, Analyst, 2012, 137, 944–952.

5 A. T. E. Vilian, M. Rajkumar, S. M. Chen, C. C. Hu and S. Piraman, RSC Adv., 2014, 4, 48522–48534.

6 B. Kaur and R. Srivastava, Electroanalysis, 2014, 26, 1739–1750.

7 H. Wang, Y. Wu and X. Yan, Anal. Chem., 2013, 85, 1920–1925.

8 A. J. S. Ahammad, M. M. Rahman, G. Xu, S. Kim and J. Lee, Electrochim. Acta, 2011, 56, 5266–5272.

9 M. A. Ghanem, Electrochem. Commun., 2007, 9, 2501–2506.

10 A. Kumar and A. Pamwar, Microchim. Acta, 1993, 111, 177–182.

11 S. P. Wang and T. H. Huang, Anal. Chim. Acta, 2005, 534, 207–214.

12 P. Nagaraja, R. A. Vasantha and K. R. Sunitha, Talanta, 2011, 55, 1039–1046.

13 W. Zhang, D. L. Lin, Z. X. Zou and Y. Q. Li, Talanta, 2007, 71, 1481–1486.

14 J. T. Han, K. J. Huang, J. Li, Y. M. Liu and M. Yu, Colloid. Surface B, 2012, 98, 58–62.

15 M. Amiri, S. Ghaffari, A. Bezaatpour and F. Marken, Sens. Actuators, B, 2012, 162, 194–200.

16 W. Xiong, M. Wu, L. Zhou and S. Liu, RSC Adv., 2014, 4, 32092–32099.

17 K. J. Huang, Y. J. Liu, H. B. Wang, Y. Y. Wang and Y. M. Liu, Biosens. Bioelectron., 2014, 55, 195–202.

18 M. A. Guillorn, T. E. McKnight, A. Melechko, V. I. Merkulov, P. F. Britt, D. W. Austin, D. H. Lowndes and M. L. Simpson, J. Appl. Phys., 2002,91, 3824–3828.

19 X. R. Wang, X. L. Li, L. Zhang, Y. K. Yoon, P. K. Weber, H. L. Wang, J. Guo and H. J. Dai, Science, 2009, 324, 768–771.

20 X. M. Chen, G. H. Wu, Y. Q. Jiang, Y. R. Wang and X. Chen, Analyst, 2011, 136, 4631–4640.

21 L. A. Mashat, K. Shin, K. Kalantar-zadeh, J. D. Plessis, S. H. Han, R. W. Kojima, R. B. Kaner, D. Li, X. Gou, S. J. Ippolito and W. Wlodarski, J. Phys. Chem. C, 2010, 114, 16168–16173.

22 K. J. Huang, L. Wang, H. B. Wang, T. Gan, Y. Y. Wu, J. Li and Y. M. Liu, Talanta, 2013, 114, 43–48.

23 H. Yu, C. Ma, B. Ge, Y. Chen, Z. Xu, C. Zhu, C. Li, Q. Ouyang, P. Gao, J. Li, C. Sun, L. Qi, Y. Wang and F. Li, Chem-Eur. J, 2013, 19, 5818–5823.

24 Q. Li, B. Guo, J. Yu, J. Ran, B. Zhang, H. Yan and J. R. Gong, J. Am. Chem. Soc., 2011, 133, 10878–10884

25 X. Chen, X. J. Huang, L. G. Kong, Z. Guo, X. C. Fu, M. Q. Li and J. H. Liu, J. Mater. Chem., 2010, 20, 352–359.

26 L. Sheeney-Haj-Ichia, J. Wasserman and I. Willner, Adv. Mater., 2002, 14, 1323–1326.

27 I. Willner, F. Patolsky and J. Wasserman, Angew. Chem., Int. Ed., 2001, 40, 1861–1864.

28 B. X. F. Wang, Y. Zhou, J. J. Xu and H. Y. Chen, Adv. Funct. Mater. 2009, 19, 1444–1450.

29 W. S. Hummers and R. E. Offeman, J. Am. Chem. Soc., 1958, 80, 1339–1339.

30 A. C. Ferrari, J. C. Meyer and V. Scardaci, Phys. Rev. Lett., 2006, 97, 7404–7410.

31 Y. Zhu, S. Murali, W. Cai, X. Li, J. W. Suk, J. R. Potts and R. S. Ruoff, Adv. Mater., 2010, 35, 3906–3924.

32 A. Martín, J. Hernández-Ferrer, L. Vázquez, M. T. Martínez and A. Escarpa, RSC Adv., 2014, 4, 132–139.

33 S. Park and R. S. Ruoff, Nat. Nanotechnol., 2009, 4, 217–224.

34 S. Zhang, S. Tang, J. Lei, H. Dong and H. Ju, J. Electroanal. Chem., 2011, 656, 285–288.

35 X. Chen, H. Ye, W. Wang, B. Qiu, Z. Lin and G. Chen, Electroanal., 2010, 22, 2347–2352.

36 B. Z. Fan , J. Yan , L. Zhi , Q. Zhang , T. Wei , J. Feng , M. Zhang , W. Qian and F. Wei, Adv. Mater., 2010, 22, 3723–3728.

37 J. Wu, X. Shen, L. Jiang, K. Wang and K. Chen, Appl. Surf. Sci., 2010, 256, 2826–2830.

38 Q. Qu , S. Yang and X. Feng, Adv. Mater., 2011, 23, 5574–5580.

39 Y. Zhao, Y. Gao, D. Zhan, H. Liu, Q. Zhao, Y. Kou, Y. Shao, M. Li, Q. Zhuang and Z. Zhu, Talanta, 2005, 66, 51–57.

40 K. J. Huang, L. Wang, J. Li, M. Yu and Y. M. Liu, Microchim. Acta, 2013, 180, 751–757.

41 J. H. Li, D. Z. Kuang, Y. L. Feng, F. X. Zhang, Z. F. Xu and M. Q. Liu, J. Hazard. Mater. 2012, 250, 201–202.

42 K. J. Huang, L. Wang, Y. J. Liu, T. Gan, Y. M. Liu, L. L. Wang and Y. Fan, Electrochim. Acta, 2013, 107, 379–387.

43 E. Laviron, J. Electroanal. Chem., 1979, 101, 19–28.

44 N. A. Penner and P. N. Nesterenko, Analyst, 2000, 125, 1249–1254.

Figure and table captions

Scheme 1 The reaction mechanism of CdS/r-GO/GCE with dihydroxybenzene isomers.

Fig. 1 SEM images of GO (A), CdS/r-GO (B) and EDS of CdS/r-GO composite material (C).

Fig. 2 AFM images and profile line of bare of r-GO/GCE (A) and CdS/r-GO/GCE (B)

Fig. 3 CV of 0.2 mM HQ, CC and RC in pH 7.0 at (A)GCE, (B) r-GO/GCE, (C) CdS/r-GO/GCE.

Fig. 4 The oxidation peak current of 0.2 mM HQ, CC and RC on the CdS/r-GO/GCE at different pH (5.5, 6.0, 6.5, 7.0, 7.5, 8.0, 8.5) (scan rate: 0.1 V s^{-1}). Inset: the plots of E_{pa} with pH values.

Fig. 5 CV of 0.2 mM HQ, CC and RC on the CdS/r-GO/GCE at different scan rate (0.01, 0.03, 0.05, 0.075, 0.10, 0.15, 0.20, 0.25, 0.30, 0.35, 0.40 V s^{-1}). Inset: the redox peak current relation with the scan rate.

Fig. 6 (A) DPVs of HQ concentrations:0, 0.2 μM, 1.0 μM, 10 μM, 20 μM, 40 μM, 70 μM, 130 μM, 190 μM, 250 μM, 340 μM, 450 μM, 580 μM, 700 μM, 850 μM, 1000 μM (B) DPVs of CC concentrations: 0, 0.5 μM, 5 μM, 15 μM, 40 μM, 60 μM, 160 μM, 280 μM, 460 μM, 700μM, 1000 μM, 1350 μM and (C) DPVs of RC concentrations: 0, 1 μM, 5 μM, 15 μM, 25 μM, 60 μM, 100 μM, 180 μM, 300 μM, 500μM at CdS/r-GO/GCE in the presence of other two interfering substance (concentration 0.2 μM).

Fig. 7 CV of 0.2 mM HQ, CC and RC recorded on the CdS/r-GO/GCE with increasing time.

Table 1 Comparison of different electrochemical sensors for the determination of dihydroxybenzene isomers.

Table 2 Results of determination of dihydroxybenzene isomers in the real samples.

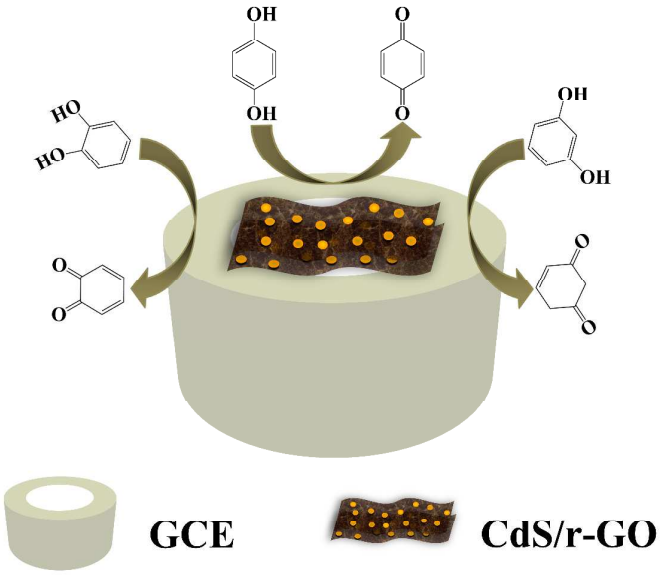

Scheme 1

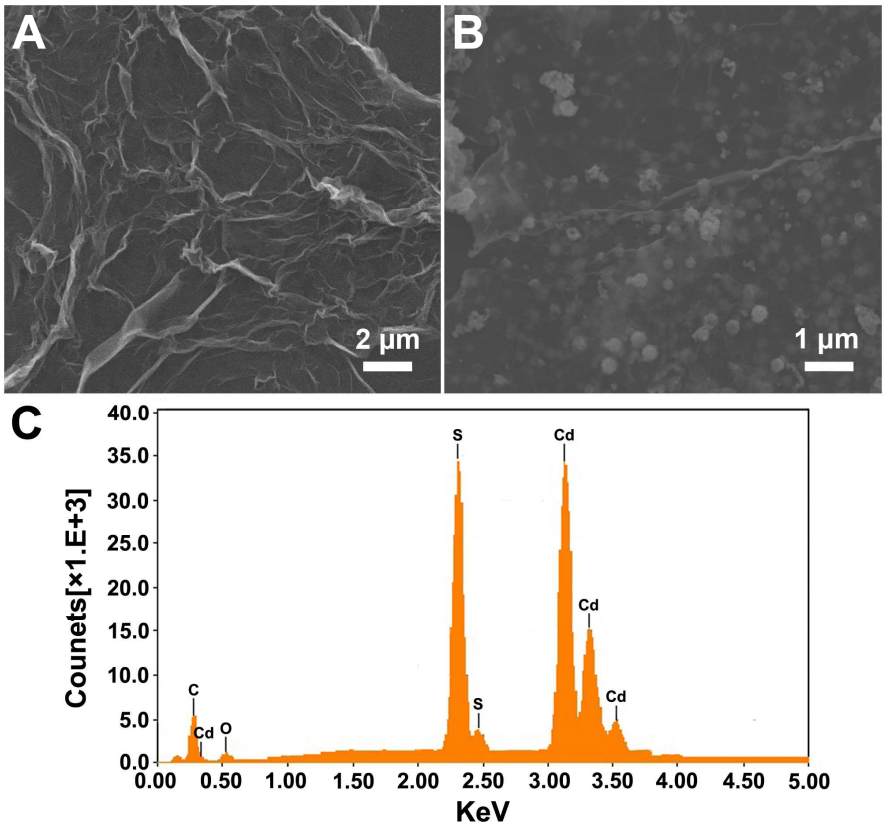

Fig. 1

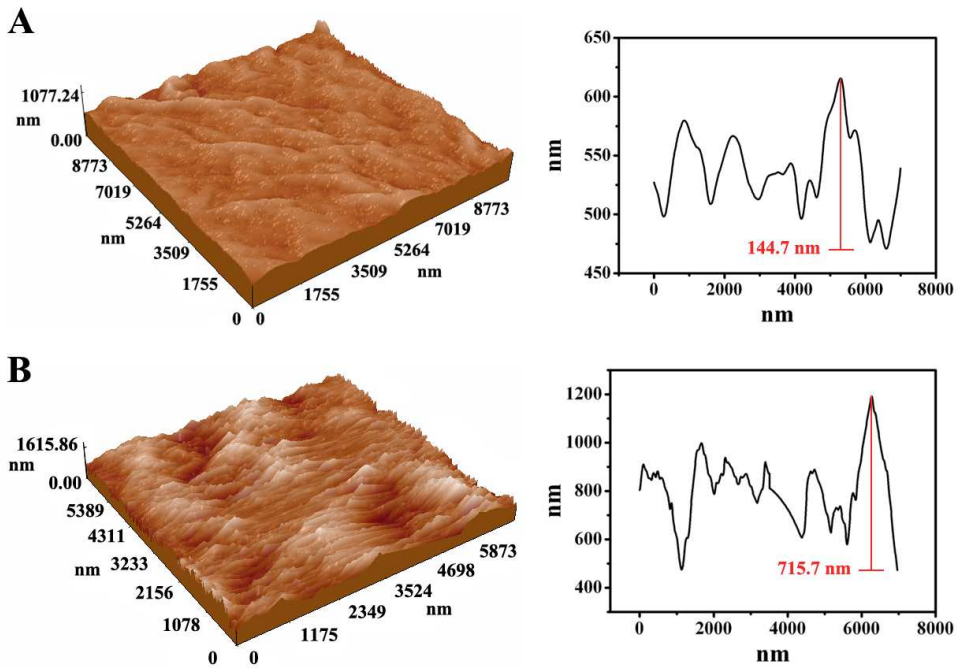

Fig. 2

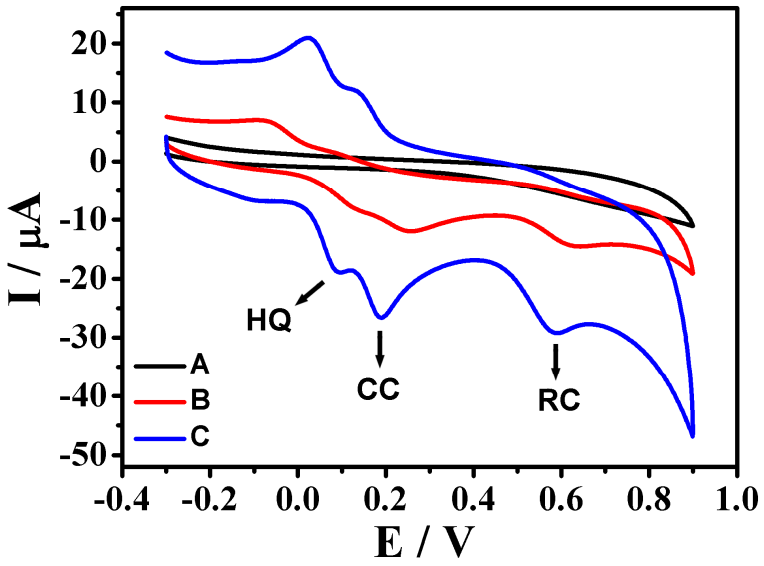

Fig. 3

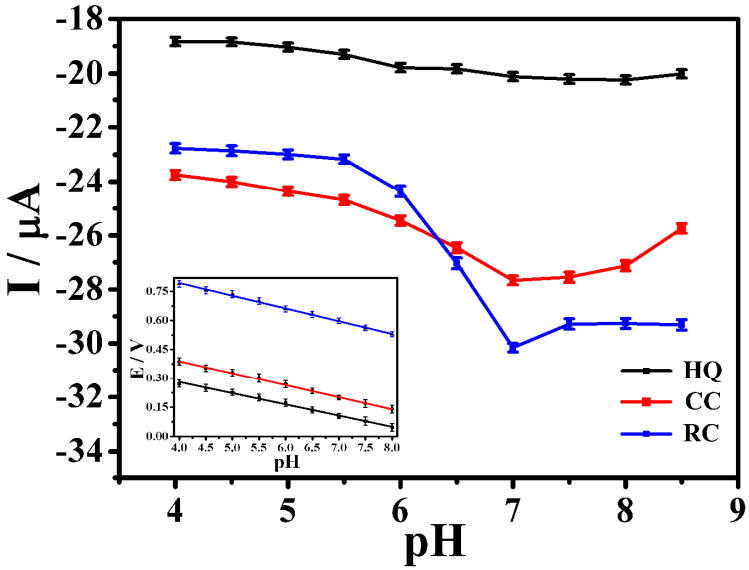

Fig. 4

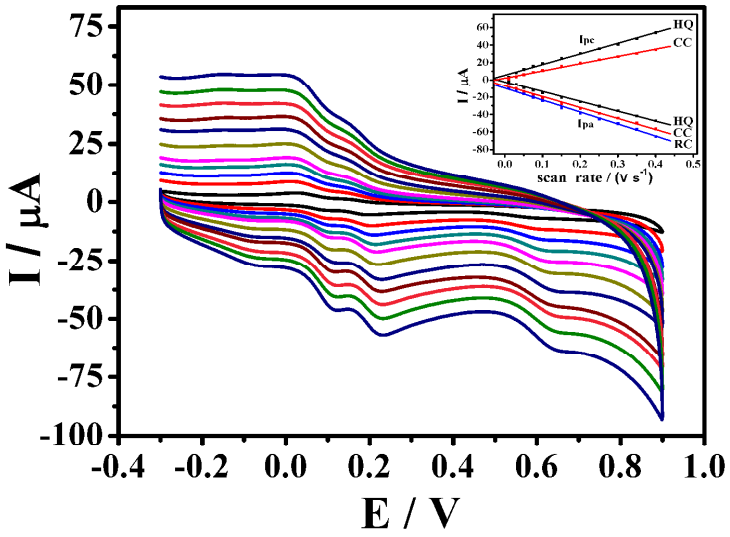

Fig. 5

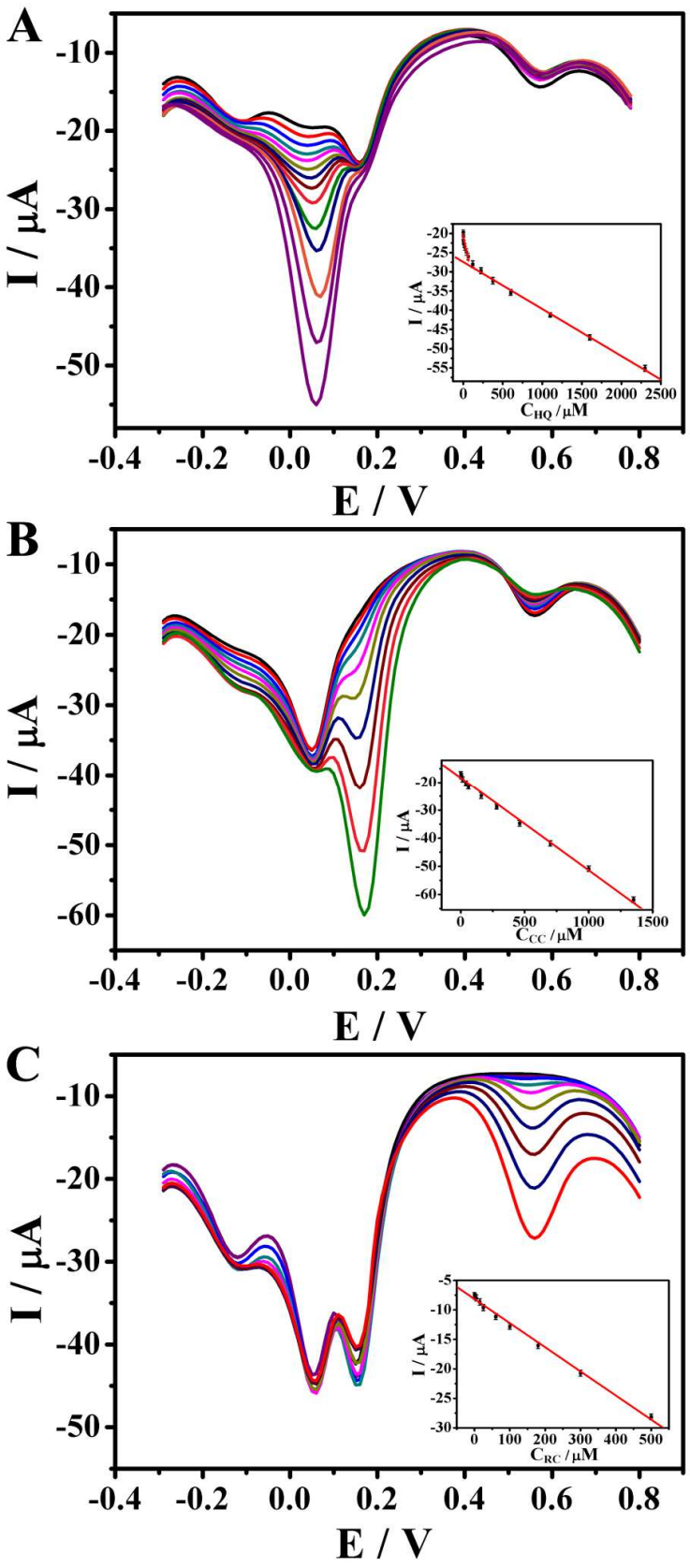

Fig. 6

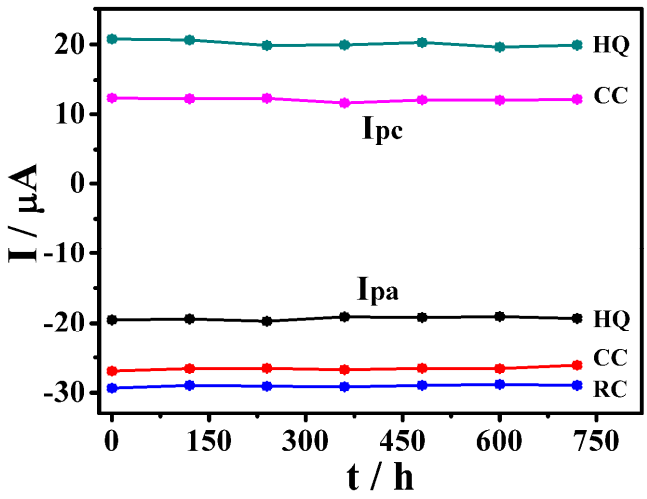

Fig. 7

Electrode	Linear (μM)			Detection limit (μM)			Ref.
	HQ	CC	RC	HQ	CC	RC	
pyridinic-NG/GCE	5.0-200	5.0-200	—	0.38	1	—	3
graphene-chitosan/GCE	1.0-400	1.0-550	1.0-300	0.75	0.75	0.75	7
PTH/GCE	0.5-25	100-200	—	0.03	0.025	—	8
CNP-chitosan/GCE	0.8-100	0.8-100	8.0-1000	0.2	0.2	3	15
AgNPs-Pdop@Gr/GCE	—	0.5-240	—	—	0.1	—	40
WS_2-Gr/GCE	1-100	1-100	1-100	0.1	0.2	0.1	42
CdS/r-GO/GCE	0.2-2300	0.5-1350	1.0-500	0.054	0.09	0.23	This work

Table 1

samples	original(μM)	Added (μM)			Found (μM)			Recovery(%)		
		HQ	CC	RC	HQ	CC	RC	HQ	CC	RC
Tap water	-	50	50	50	50.3 ± 0.7	49.6±0.5	50.9±0.8	100.9	98.6	102.8
		100	100	100	99.2±0.5	100.9±0.6	100.7±0.9	98.9	101.4	101.6
Well water	-	50	50	50	50.6 ± 0.5	50.9±0.4	49.3±0.8	101.9	102.2	97.8
		100	100	100	100.6±0.3	98.9±0.7	101.5±1.1	100.8	98.6	102.1
River water	-	50	50	50	49.3 ± 0.7	50.4±0.5	48.8±1.0	98.1	101.8	96.8
		100	100	100	100.2±0.5	100.9±0.4	98.7±1.2	100.5	101.2	98.3

Table 2